A new accurate residual-based a posteriori error indicator for the BEM in 2D-acoustics

Marc Bakry, Sebastien Pernet, Francis Collino

Computers and Mathematics with Applications 73 (2017) 2501–2514

Contents lists available at ScienceDirect

Computers and Mathematics with Applications

journal homepage: www.elsevier.com/locate/camwa

A new accurate residual-based a posteriori error indicator for the BEM in 2D-acoustics

Marc Bakry [a,*], Sébastien Pernet [b], Francis Collino [c]

[a] INRIA Saclay — Ile de France, bâtiment Alan Turing, 1 rue Honoré d'Estienne d'Orves, Campus de l'Ecole Polytechnique, FR-91120 Palaiseau, France

[b] Office National d'Etudes et de Recherches Aérospatiales (ONERA), Département Traitement de l'Information et Modélisation (DTIM), 2 avenue Edouard Belin, FR-31055 Toulouse Cedex 4, France

[c] CERFACS, 42 avenue Gaspard Coriolis, FR-31057 Toulouse Cedex 1, France

ARTICLE INFO

Article history:
Received 12 April 2016
Received in revised form 7 March 2017
Accepted 13 March 2017
Available online 2 May 2017

Keywords:
A posteriori error estimate
Adaptive boundary element method
Auto-adaptive refinement
Helmholtz equation
Oscillating integrals
2D-acoustics

ABSTRACT

In this work we construct a new reliable, efficient and local *a posteriori* error estimate for the single layer and hyper-singular boundary integral equations associated to the Helmholtz equation in two dimensions. It uses a localization technique based on a generic operator Λ which is used to transport the residual into L^2. Under appropriate conditions on the construction of Λ, we show that it is asymptotically exact with respect to the energy norm of the error. The single layer equation and the hyper-singular equation are treated separately. While the current analysis requires the boundary to be smooth, numerical experiments show that the new error estimators also perform well for non-smooth boundaries.

1. Introduction

The Boundary Element Method (BEM) is a method, based on boundary integral formulations, that can be used for the resolution of wave propagation problems. It features strong advantages since only the boundary Γ of the domain is meshed, the radiation condition at infinity is intrinsically taken into account and it is more accurate than other common methods like the Finite Element Method (FEM). The main disadvantages of the BEM are the difficult implementation (singular integrals) and the manipulation of fully populated matrices. This last problem has been partially bypassed thanks to recent improvements on the acceleration of the BEM like the Fast Multipole Method [1] or $\mathcal{H}$-matrices [2].

In this paper we study the propagation of an acoustic wave with wave number k in an infinite medium. This wave is diffracted by a scatterer represented by a simply-connected bounded Lipschitz domain with boundary Γ. In the following, a discretization of this boundary will be named $\mathcal{T}_h$. We apply either a Dirichlet boundary condition for the global field u such that $u|_\Gamma = 0$ or a Neumann boundary condition $\frac{\partial u}{\partial n}\big|_\Gamma = 0$ where n is the outward pointing normal of the scatterer. The two integral equations we are going to study are

$$(\mathcal{S}_k\varphi)(x) := \int_\Gamma G_k(x,y)\,\varphi(y)\,d\gamma_y = -u_i(x), \tag{1}$$

* Corresponding author.
E-mail addresses: marc.bakry@gmail.com (M. Bakry), sebastien.pernet@onera.fr (S. Pernet), francis.collino@orange.fr (F. Collino).

http://dx.doi.org/10.1016/j.camwa.2017.03.016
0898-1221/

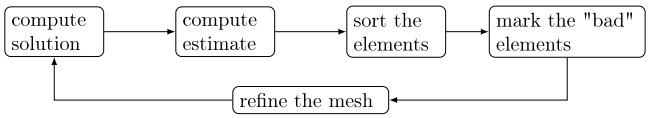

Fig. 1. Example of an algorithm for autoadaptive mesh-refinement.

which solves the scattering problem with Dirichlet boundary condition and

$$(\mathcal{N}_k\psi)(x) := \text{f.p.} \int_\Gamma \frac{\partial^2 G_k}{\partial n_x \partial n_y}(x,y)\,\psi(y)\,d\gamma_y = -\partial_n u_i(x), \tag{2}$$

which solves the scattering problem with a Neumann boundary condition for an incoming wave u_i and is given as a finite parts integral. The kernel G_k is the Green function associated to the Helmholtz equation. For 2D wave propagation problems, it reads

$$G_k(x,y) = \frac{i}{4} H_0^{(1)}(k|x-y|),$$

with $H_0^{(1)}$ the Hankel function of the first kind and of order 0.

The operator $\mathcal{S}_k$ is named *single layer integral operator* and the operator $\mathcal{N}_k$ is commonly named *hyper-singular operator*. These equations are solved using a Galerkin method. The variational formulations are recalled (see [3]) below:

- Eq. (1), find $\varphi \in H^{-1/2}(\Gamma)$ such that for all $\varrho \in H^{-1/2}(\Gamma)$,

$$\int_\Gamma \int_\Gamma \varrho(x)\, G_k(x,y)\, \varphi(y)\, d\gamma_x\, d\gamma_y = -\int_\Gamma \varrho(x)\, u_i(x)\, d\gamma_x, \tag{3}$$

- Eq. (2), find $\psi \in H^{1/2}(\Gamma)$ such that for all $\varsigma \in H^{1/2}(\Gamma)$,

$$\int_\Gamma \int_\Gamma \overrightarrow{\text{rot}}_\Gamma \varsigma(x)\, G_k(x,y)\, \overrightarrow{\text{rot}}_\Gamma \psi(y)\, d\gamma_x\, d\gamma_y - k^2 \int_\Gamma \int_\Gamma \varsigma(x)\, G_k(x,y)\, \psi(y)\, n_x \cdot n_y\, d\gamma_x\, d\gamma_y = -\int_\Gamma \varsigma(x)\, \partial_n u_i(x)\, d\gamma_x. \tag{4}$$

Despite its strong advantages, the BEM for wave propagation problems still lacks reliable, efficient and automatic tools for the control of the error. Such tools are called *a posteriori error estimates*. They are used in the context of *auto-adaptive refinement* in order to ensure the accuracy of a computation. An auto-adaptive loop for mesh refinement can be described as pictured in Fig. 1.

Three properties are required. Let η be such an estimate and e_h the numerical error, it must be *reliable* and *efficient*, *i.e.*, there exist two constants $C_{\text{rel}}, C_{\text{eff}} > 0$ such that

$$C_{\text{eff}}\,\eta \le \|e_h\| \le C_{\text{rel}}\,\eta.$$

The third property is the *locality* of η. It means that the total value of the estimate can be decomposed as the sum of local contributions of the estimate. This can be expressed by

$$\eta^2 = \sum_{\tau \in \mathcal{T}_h} \eta_\tau^2$$

where η_τ represents the value of η restricted to τ. This definition *does not imply* any local efficiency with respect to the error! Here we only mean that we need some value which can be defined locally in order to guide an autoadaptive refinement loop.

A posteriori estimates for the BEM have already been widely investigated, although not as much as for the FEM. Moreover, the numerical analysis remains to our knowledge rather limited. We can cite the pioneering work of B. Faermann [4–6] which is based on the localization of the norms associated to Sobolev spaces of non-integer order on patches of elements of the mesh. In the field of acoustic scattering, we can have a look at the multilevel error indicator in [7] for general Fredholm operators. There is also the work of Chen et al. [8] in acoustics where a simple residual-based error estimate is used. Some investigations in electromagnetism have been made. For example Nochetto and Stamm [9] developed a weighted residual-based error estimate for the Electric Field Integral Equation. Finally, the most successful work (to our knowledge) is the one of the team of D. Praetorius at TU Wien and its collaborators who have deeply studied the *a posteriori* error estimates and the adaptive methods in the context of BEM for the Laplace problems. The first examples [10,11] use the fact that the norm of the residual is an equivalent norm of the error. They are based on a localization of this norm. Other examples (the list being clearly non-exhaustive) are the averaging error estimates [12,13] featuring hierarchical meshes and localizations of the Sobolev norms. A nice review of most of the existing estimates can be found in [14]. For some of the estimates (for example [10]), there exists a proof for quasi-optimal convergence rates [15]. The topic of optimal convergence

of autoadaptive refinement algorithms is tackled using an abstract setting in [16] and will not be further recalled in this paper.

The process of localization induces generally a loss of control between the "value of the error" and the value of the estimate. The corresponding multiplicative constant (equivalently named *efficiency constant*) will essentially depend on Γ. We seek a way to set the value of this constant independently on Γ while keeping the three first properties. The result is a new error estimate which features a localization technique based on the use of a localization operator Λ. Under appropriate conditions (in particular if Γ is $\mathcal{C}^\infty$), it is asymptotically exact with respect to the Galerkin norm of the error in the sense that when the mesh is refined it reflects the value of the error up to a higher order term. In the case of acoustic scattering and more particularly Eqs. (1) and (2), the estimates read as follows: For r_h the residual of the equation which is solved,

$$\eta_{\mathcal{S}_0} = \|\Lambda_{\mathcal{S}_0} r_h\|_0 \quad \text{and} \quad \eta_{\mathcal{N}_0} = \|\Lambda_{\mathcal{N}_0} r_h\|_0,$$

with

$$\Lambda_{\mathcal{S}_0} r_h(x) := \frac{2}{\sqrt{\pi}} \nabla_\Gamma \cdot \int_\Gamma \sqrt{|x-y|}\, \nabla_\Gamma r_h(y)\, d\gamma_y,$$

and

$$\Lambda_{\mathcal{N}_0} r_h(x) := \frac{1}{\sqrt{\pi}} \int_\Gamma \frac{r_h(y)}{\sqrt{|x-y|}}\, d\gamma_y.$$

The paper is organized as follows. We first give an abstract setting. We then make a simple observation which is the first step to the construction of the new *a posteriori* error estimate. We state the theorem defining the estimate and we suggest a method for its construction. We build the estimates corresponding to the Eqs. (1) and (2). We conclude with two numerical examples in order to confirm the expected properties and we give an opening on another way to build the operators Λ.

2. Abstract setting

In this section we establish the abstract setting which we are going to use. We also *slightly change the notations for the error and the residual.*

The equations resulting from the BEM are of the form

$$\mathcal{A}u = b, \tag{5}$$

where $\mathcal{A} : H \to H^\star$ is a linear bounded operator, H is some separable Hilbert space and $H^\star$ its topological dual space. We denote by $\|\cdot\|_H$ the norm on H which is based upon the inner product $(\cdot,\cdot)_H$.

We write $(\cdot,\cdot)$ for the L^2 inner product and $\langle\cdot,\cdot\rangle$ for the classical duality brackets.

In the following, for any operator $\mathcal{L}$ the adjoint operator is written $\mathcal{L}^\star$.

In this paper we are interested in the class of linear *Fredholm* operators which can be decomposed in the form

$$\mathcal{A} = \mathcal{A}_0 + \mathcal{K}, \tag{6}$$

where $\mathcal{A}_0$ is the continuous, symmetric, and coercive part and $\mathcal{K}$ is a compact perturbation. The Fredholm alternative [17] yields a solvability criterion for (5) and we suppose that this problem admits a unique solution. The coercive part $\mathcal{A}_0$ allows us to define the *Galerkin norm.*

Proposition 2.1 (*Galerkin Norm*)**.** *Using the notation of* (6)*, the quantity* $|||u|||^2 = \langle \mathcal{A}_0 u, u\rangle$ *defines an equivalent norm to* $\|\cdot\|_H$ *on the Hilbert space H. This norm is called the Galerkin norm.*

Proof. The proof is trivial since the operator $\mathcal{A}_0$ is bounded and coercive on H. □

In this paper we do not concern ourselves with the convergence of the autoadaptive algorithm but only on the *a posteriori* error estimation. Consequently, we suppose that the autoadaptive algorithm produces a sequence $(\mathcal{T}_l)_{l\in\mathbb{N}}$ of successively refined meshes and corresponding nested approximation spaces $V_l \subset V_{l+1} \subset H$ such that

$$V_\infty := \overline{\bigcup_{l=0\ldots\infty} V_l} = H. \tag{7}$$

Remark 2.1. We do *not necessarily* have $V_\infty = H$ when we use a standard autoadaptive algorithm like the so-called Dörfler marking strategy [16]. Nevertheless, the paper [18] proposes a simple modification of the latter which does not impact the optimal convergence of the algorithm and ensures the property (7).

We suppose furthermore that for each $l \in \mathbb{N}$ the associated discrete problem is well-posed. The corresponding discrete solution is written u_l and satisfies $\langle \mathcal{A}u_l, v_l\rangle = \langle b, v_l\rangle$ for all $v_l \in V_l$. The *approximation error* is then

$$e_l = u - u_l.$$

We also suppose that $\|\!|u - u_l|\!\| \xrightarrow[l\to\infty]{} 0$, *i.e.*, the discrete solution u_l converges to the *exact* solution u of (5). In practice, all these assumptions are satisfied if the mesh $\mathcal{T}_0$ corresponding to the initial space V_0 is sufficiently fine. However, [18] shows that some assumptions still hold if the initial mesh is coarse.

We define the *residual*

$$r_l = b - \mathcal{A}u_l, \quad r_l \in H^\star. \tag{8}$$

Finally, for sake of simplicity in the presentation, we assume that for all $l \in \mathbb{N}$, $u_l \neq u$.

We introduce finally the notion of *higher order term* which we will extensively use in the following.

Definition 2.1 (*Higher Order Term*)**.** We say that a function $a(\cdot)$ depending on b is a *higher order term* compared to b in 0 if

$$\lim_{b\to 0} \frac{a(b)}{b} = 0.$$

In particular, *higher order terms* are often, in the following, a consequence of some compact operator applied to "something" converging to zero, typically the error e_l. In fact, we have the two following lemmas.

Lemma 2.1. *Let $(w_l)_{l\in\mathbb{N}}$ be the sequence defined as*

$$w_l = \frac{e_l}{\|\!|e_l|\!\|}, \quad l \in \mathbb{N},$$

then $(w_l)_{l\in\mathbb{N}}$ is bounded and converges weakly to zero in V_∞.

Proof. We follow the same pattern as the proof of Lemma 6 in [19].

We prove the result by using the following argument: if there exists $w \in H$ such that for every subsequence $(z_{k_l})_{l\in\mathbb{N}}$ of a sequence $(z_l)_{l\in\mathbb{N}}$, there exists a subsequence of these subsequences which converges weakly to w, then $(z_l)_{l\in\mathbb{N}}$ converges weakly to w.

Any subsequence of the sequence $(w_l)_{l\in\mathbb{N}}$ is obviously bounded since for all $l \in \mathbb{N}$, $\|\!|w_l|\!\| = 1$. Consequently, there exists for each of these subsequences, a weakly convergent subsequence $(w_{l_j})_{j\in\mathbb{N}}$ converging to some w. We want to prove that $w = 0$.

On the other side, the Galerkin orthogonality of the error $\langle \mathcal{A}e_l, v_l\rangle = 0$ for all $v_l \in V_l$ and the nestedness of the subspaces V_l implies that for all $j \in \mathbb{N}$ such that $l_j \geq l$, we have for all $v_l \in V_l$

$$\begin{aligned}\langle \mathcal{A}w_{l_j}, v_l\rangle &= \|\!|u - u_{l_j}|\!\|^{-1} \langle \mathcal{A}e_{l_j}, v_l\rangle \\ &= 0\end{aligned}$$

Moreover, for all $\varepsilon > 0$, there exists $j_0 \in \mathbb{N}$ such that for all $j \geq j_0$, we have $l_j \geq l$ and $|\langle \mathcal{A}(w - w_{l_j}), v_l\rangle| \leq \varepsilon$ by using the weak convergence of $(w_{l_j})_{j\in\mathbb{N}}$ to w and the continuity of the linear operator $\mathcal{A}$. Therefore, we have for all $\varepsilon > 0$, for all $l \in \mathbb{N}$, and sufficiently large l_j that

$$|\langle \mathcal{A}w, v_l\rangle| = \langle \mathcal{A}(w - w_{l_j}), v_l\rangle + \langle \mathcal{A}w_{l_j}, v_l\rangle \leq 0 + \varepsilon = \varepsilon,$$

which implies that for all $l \in \mathbb{N}$, we have

$$\langle \mathcal{A}w, v_l\rangle = 0, \quad \forall v_l \in V_l.$$

Now, by density and continuity, the hypothesis (7) leads to

$$\langle \mathcal{A}w, v\rangle = 0, \quad \forall v \in H.$$

Finally, the invertibility of the operator $\mathcal{A}$ gives $w = 0$ and the sequence $(w_l)_l$ converges weakly to $w = 0$. □

We then have the following lemma which enlightens the reason why compact operators can yield higher order terms.

Lemma 2.2. *If $\widetilde{\mathcal{K}} : H \to H^\star$ is a compact operator, then $\langle \widetilde{\mathcal{K}}e_l, e_l\rangle$ gives rise to a higher order term compared to $\|\!|e_l|\!\|^2$.*

Proof. Let $(w_l)_{l\in\mathbb{N}}$ be the sequence defined in Lemma 2.1. We know that this sequence converges weakly to 0. As a consequence, using the fact that $\widetilde{\mathcal{K}}$ is compact, we have the following strong convergence in $H^\star$

$$\|\widetilde{\mathcal{K}}w_l\|_{H^\star} \xrightarrow[l\to\infty]{} 0.$$

Finally, using Proposition 2.1, there exists a constant $C > 0$ such that for all $v \in H$, $\|v\|_H \leq C\|\!|v|\!\|$ and we can write:

$$\begin{aligned}|\langle \widetilde{\mathcal{K}}e_l, e_l\rangle| &= \|\!|e_l|\!\| \, |\langle \mathcal{K}w_l, e_l\rangle| \\ &\leq C\|\widetilde{\mathcal{K}}w_l\|_{H^\star} \, \|\!|e_l|\!\|^2\end{aligned}$$

which means in particular that $\frac{|\langle \widetilde{\mathcal{K}}e_l, e_l\rangle|}{\|\!|e_l|\!\|^2} \xrightarrow[l\to\infty]{} 0$. □

3. Construction of a new *a posteriori* error estimate

The aim of this section is to build a new efficient, reliable, local and possibly asymptotically exact (with respect to the Galerkin norm of the error) *a posteriori* error estimate in the sense of exactness up to some higher order terms.

As for many estimates of the literature (for example [10]), we use the fact that under the assumption that Eq. (5) is well-posed, the norm of the residual $\|r_l\|_{H^\star}$ is a reliable and efficient *a posteriori* error estimate of the norm of the error $|||e_l|||$. Actually, the well-posedness character of the continuous problem implies the existence of an inf–sup condition, *i.e.*, there exists $\alpha > 0$ such that

$$\inf_{v\in H}\sup_{w\in H}\frac{|\langle \mathcal{A}v, w\rangle|}{\|v\|_H\|w\|_H} \geq \alpha.$$

In particular, for all $u_l \in V_l$ (not necessarily solution of the Galerkin problem), we have:

$$\|r_l\|_{H^\star} = \sup_{w\in H}\frac{|\langle \mathcal{A}(u-u_l), w\rangle|}{\|w\|_H} \geq \alpha\|u-u_l\|_H.$$

Finally, the continuity of $\mathcal{A}$ leads to $\|r_l\|_{H^\star} \leq \|\mathcal{A}\|\|u-u_l\|_H$ and we have

$$\|A\|^{-1}\|r_l\|_{H^\star} \leq \|u-u_l\|_H \leq \alpha^{-1}\|r_l\|_{H^\star}. \tag{9}$$

We have the following theorem.

Theorem 3.1 (*New Estimate-Strong Form*). *Let $\Lambda : H^\star \to L^2(\Gamma)$ be an isomorphism. Then, the a posteriori error estimate defined by*

$$\eta_\Lambda = \|\Lambda r_l\|_0,$$

is reliable, efficient and local (following our definition given in the introduction).

Proof. Since Λ is an isomorphism, then Λ and Λ^{-1} are bounded and we have $\|\Lambda^{-1}\|\|r_l\|_{H^\star} \leq \eta_\Lambda \leq \|\Lambda\|\|r_l\|_{H^\star}$. Consequently, $\|\Lambda r_l\|_0$ is a reliable and efficient *a posteriori* error estimate of $\|r_l\|_{H^\star}$. We conclude by using (9). □

In the following we discuss the possible asymptotic exactness of the estimate introduced in Theorem 3.1 with respect to the Galerkin norm of the error.

We have the following proposition.

Proposition 3.1. *Let η_Λ be the estimate introduced in Theorem 3.1. If there exists an operator Λ such that $\Lambda^\star\Lambda\mathcal{A}_0 = \mathcal{I} + \mathcal{K}_2$ where $\mathcal{I}$ is the identity operator and $\mathcal{K}_2 : H \to H$ some compact perturbation, then η_Λ is asymptotically exact with respect to the Galerkin norm of the error.*

Proof. Let us start from the definition of $\|\Lambda r_l\|_0^2$: using the decomposition of $\mathcal{A}$ as the sum of a coercive part $\mathcal{A}_0$ and a compact part $\mathcal{K}$, we have

$$\begin{aligned}\|\Lambda r_l\|_0^2 &= (\Lambda\mathcal{A}e_l, \Lambda\mathcal{A}e_l)\\ &= (\Lambda(\mathcal{A}_0+\mathcal{K})e_l, \Lambda(\mathcal{A}_0+\mathcal{K})e_l)\\ &= (\Lambda\mathcal{A}_0e_l, \Lambda\mathcal{A}_0e_l) + (\Lambda\mathcal{K}e_l, \Lambda\mathcal{A}_0e_l) + (\Lambda\mathcal{A}_0e_l, \Lambda\mathcal{K}e_l) + (\Lambda\mathcal{K}e_l, \Lambda\mathcal{K}e_l)\\ &= \langle \mathcal{A}_0e_l, \Lambda^\star\Lambda\mathcal{A}_0e_l\rangle + \langle \mathcal{K}_1e_l, e_l\rangle,\end{aligned} \tag{10}$$

where $\mathcal{K}_1 = \mathcal{A}_0^\star\Lambda^\star\Lambda\mathcal{K} + \mathcal{K}^\star\Lambda^\star\Lambda\mathcal{A}_0 + \mathcal{K}^\star\Lambda^\star\Lambda\mathcal{K}$ is a compact operator from H to $H^\star$ as the composition of bounded and compact operators.

If $\Lambda^\star\Lambda\mathcal{A}_0 = \mathcal{I} + \mathcal{K}_2$, the identity (10) becomes

$$\begin{aligned}\|\Lambda r_l\|_0^2 &= \langle \mathcal{A}_0e_l, e_l\rangle + \langle(\mathcal{K}_1 + \mathcal{K}_2^\star\mathcal{A}_0)e_l, e_l\rangle\\ &= |||e_l|||^2 + \langle \mathcal{K}_3e_l, e_l\rangle,\end{aligned} \tag{11}$$

where the operator $\mathcal{K}_3 = \mathcal{K}_1 + \mathcal{K}_2^\star\mathcal{A}_0 : H \to H^\star$ is compact. Using Lemma 2.2 with $\mathcal{K}_3$, we have that the quantity $\delta_l := \langle \mathcal{K}_3e_l, e_l\rangle/|||e_l|||^2$ converges to zero when $l \to +\infty$ and the equality (11) leads to

$$\frac{\|\Lambda r_l\|_0^2}{|||e_l|||^2} = 1 + \delta_l \xrightarrow[l\to+\infty]{} 1. \tag{12}$$

In other words, by carefully choosing Λ, the corresponding estimate η_Λ is asymptotically exact with respect to the Galerkin norm of the error. □

The last remaining question is: how do we choose Λ? In many applications of the BEM, H and $H^\star$ are Sobolev spaces such that

$$H = H^s(\Gamma) \quad \text{and} \quad H^\star = H^{-s}(\Gamma), \quad s \in \mathbb{R}$$

which means that $\mathcal{A}_0$ is an operator of order $2s$. The operator Λ is consequently of order $-s$: it is an "approximation of the inverse of the square root of $\mathcal{A}_0$". In a way, this problem is really close to analytical preconditioning techniques [20,21] where one is looking for an approximate inverse of $\mathcal{A}$.

Such an operator Λ is not easily build and we suggest here an approach based on *microlocal analysis*. We perfectly acknowledge the fact that microlocal analysis techniques require Γ to be $\mathcal{C}^\infty$. That leads us to the following remark.

Remark 3.1 (*Important!*)**.** The analysis we will be conducting in the following *requires* Γ to be $\mathcal{C}^\infty$. However, this is almost never the case in practice. In fact, the analysis will help us to find *candidates* for Λ which will have the required properties on such boundaries. Once we selected a potential candidate, there are no objections to trying it for domains with singularities or general Lipschitz boundaries. We are just not sure of the expected properties. This is what will be done in the numerical applications.

On $\mathcal{C}^\infty$ surfaces/contours, $\mathcal{A}$ is a *pseudo-differential operator*. The *class of symbols of* $\mathcal{A}$ may be seen as the set of all its Fourier representations (see [22, chapters 6–8], for all the details). There is at least one representative of this class whose expansion is a sum of pseudo-homogeneous terms. The leading term is called *principal homogeneous symbol* $\sigma^0_{\mathcal{A},q}$ and its degree of homogeneity q yields the differentiation order of $\mathcal{A}$. The principal homogeneous symbol of $\mathcal{A}_0$, homogeneous of order $2s$, is then written $\sigma^0_{\mathcal{A}_0,2s}(x,\xi)$ where ξ is a variable in the Fourier domain.

An interesting property is that we can manipulate the symbols the same way we would manipulate the operators. Consequently, the principal homogeneous symbol for the operator Λ is

$$\boxed{\sigma^0_{\Lambda,-s}(x,\xi) = \frac{1}{\sqrt{\sigma^0_{\mathcal{A}_0,2s}(x,\xi)}}}. \tag{13}$$

The knowledge of $\sigma^0_{\Lambda,-s}$ gives us an abstract candidate. We can express a representative of all the candidates as an integral operator whose kernel can be computed from $\sigma^0_{\Lambda,-s}$.

In the following section we particularize the operator $\mathcal{A}$ for Eqs. (1) and (2) and consequently the functional spaces H and $H^\star$ and the Galerkin norm $|||.|||$. We then build the corresponding operators Λ.

4. Construction of the operator Λ for two acoustic integral operators in 2D

In this section we give a method for the construction of the Λ–operator for each Eqs. (1) and (2) and compute the related explicit operators $\Lambda_{\mathcal{S}_0}$ and $\Lambda_{\mathcal{N}_0}$.

In the case of Eq. (1), we have $\mathcal{A} \equiv \mathcal{S}_k$ which means that $H = H^{-1/2}(\Gamma)$ and $H^\star = H^{1/2}(\Gamma)$. Assuming that the logarithmic capacity of Γ is lower than one, the operator $\mathcal{S}_0$ is elliptic (see [23, part 5 and 6]). The Galerkin norm may be defined as

$$|||u|||^2 = \langle \mathcal{S}_0 u, u\rangle, \quad \forall u \in H^{-1/2}(\Gamma).$$

It is known from the literature [22, p. 514], that the principal homogeneous symbol of $\mathcal{S}_0$ is

$$\sigma^0_{\mathcal{S}_0,-1}(x,\xi) = \frac{1}{2|\xi|}.$$

We deduce the principal homogeneous symbol of $\Lambda_{\mathcal{S}_0}$

$$\boxed{\sigma^0_{\Lambda_{\mathcal{S}_0},1/2}(x,\xi) = \sqrt{2|\xi|}}. \tag{14}$$

In the case of Eq. (2), we have $\mathcal{A} \equiv \mathcal{N}_k$ with $H = H^{1/2}(\Gamma)$ and $H^\star = H^{-1/2}(\Gamma)$. The Galerkin norm in this case is defined as

$$|||u|||^2 = \langle (\mathcal{N}_0 + \mathcal{S}_0)u, u\rangle, \quad \forall u \in H^{1/2}(\Gamma).$$

Once again, we find in the literature [22, p. 526], that the principal homogeneous symbol of $\mathcal{N}_0$ is

$$\sigma^0_{\mathcal{N}_0,1}(x,\xi) = \frac{|\xi|}{2}.$$

We then deduce the principal homogeneous symbol of $\Lambda_{\mathcal{N}_0}$

$$\boxed{\sigma^0_{\Lambda_{\mathcal{N}_0},-1/2}(x,\xi) = \sqrt{\frac{2}{|\xi|}}}. \tag{15}$$

The effect of the operator $\Lambda_{\mathcal{S}_0}$ can then be seen as a "half-differentiation" while the effect of the operator $\Lambda_{\mathcal{N}_0}$ is a "half-integration".

We must now re-construct a practical form of $\Lambda_{\mathcal{S}_0}$ and $\Lambda_{\mathcal{N}_0}$. We will seek these operators as integral operators as we have explicit formulas for the conversion symbol → kernel and kernel → symbol. These formulas are summarized on p. 392–394 in [22].

4.1. Construction of $\Lambda_{\mathcal{S}_0}$

The formulas for the conversion symbol → kernel are unfortunately impractical and it is easier to first guess the final form of the operator and show that it has the right symbol. Let

$$\Lambda_{\mathcal{S}_0} u(x) = -\sqrt{\pi}\ \text{f.p.} \int_\Gamma \frac{u(y)}{|x-y|^{3/2}}\, d\gamma_y, \tag{16}$$

where "f.p". means "Hadamard finite part integral". The kernel $k(x, x-y) = |x-y|^{-3/2}$ is a pseudo-homogeneous function of order $-3/2$. Using formula (7.1.82) in [22], we compute the principal homogeneous symbol of order 1/2.

$$\begin{aligned}\sigma^0_{\Lambda_{\mathcal{S}_0},1/2}(x,\xi) &= -\frac{1}{2\sqrt{\pi}}\ \text{f.p.} \int_{\mathbb{R}} k(x,z)\, e^{-i\xi z}\, d\gamma_y \\ &= -\frac{1}{2\sqrt{\pi}} \lim_{\epsilon\to 0}\left(\int_{|z|>0} \frac{e^{-i\xi z}}{|z|^{3/2}}\, dz - 2\frac{e^{-i\xi\epsilon}+e^{i\xi\epsilon}}{\sqrt{\epsilon}}\right).\end{aligned}$$

Using the fact that $\Re(e^{-i\xi z})$ is even and $\Im(e^{-i\xi z})$ is odd, we have

$$\begin{aligned}\tilde{\sigma}^0_{\Lambda_{\mathcal{S}_0},1/2}(x,\xi) &= 2\int_\epsilon^\infty \frac{\cos(\xi z)}{z^{3/2}}\, dz \\ &= 2\int_\epsilon^\infty \frac{\cos(\xi z)-1}{z^{3/2}}\, dz + \frac{4}{\sqrt{\epsilon}}.\end{aligned}$$

As $\epsilon \to 0$,

$$\begin{aligned}\sigma^0_{\Lambda_{\mathcal{S}_0},1/2}(x,\xi) &= -\frac{1}{\sqrt{\pi}}\int_0^\infty \frac{\cos(\xi z)-1}{z^{3/2}}\, dz \\ &= -\frac{1}{\sqrt{\pi}}\int_0^\infty \sqrt{|\xi|}\frac{\cos(\zeta)-1}{\zeta^{3/2}}\, d\zeta, \quad \zeta = |\xi| z\end{aligned}$$

$$\boxed{\sigma^0_{\Lambda_{\mathcal{S}_0},1/2}(x,\xi) = \sqrt{2|\xi|}}.$$

Consequently, the operator defined in (16) is a good candidate. However, we will use a slightly modified version obtained by integration by parts [24]. We set

$$\boxed{\Lambda_{\mathcal{S}_0} u(x) = \tfrac{2}{\sqrt{\pi}} \nabla_\Gamma \cdot \textstyle\int_\Gamma \sqrt{|x-y|}\, \nabla_\Gamma u(y)\, d\gamma_y}. \tag{17}$$

The kernel is modified with respect to the previous version since it contains all constant functions.

Proposition 4.1. *Let $\Gamma = \mathcal{C}_R(O)$ be the circle centered in the origin O with radius R and*

$$V = \left\{\varphi \in H^{1/2}(\Gamma),\ \langle \varphi, 1_\Gamma\rangle = 0\right\}$$

the subspace of all functions of $H^{1/2}(\Gamma)$ with zero mean, then the operator

$$\Lambda_{\mathcal{S}_0} : V \to L^2(\Gamma)$$

defined in (17) is an isomorphism.

Proof. The operator $\Lambda_{\mathcal{S}_0}$ is Fredholm since it corresponds, by construction, to $\mathcal{S}_0^{-1/2}$ up to more regular operators which are obviously compact as a consequence of the Sobolev embeddings. Consequently, we only need to prove that $\Lambda_{\mathcal{S}_0}$ is injective. We will show that the only eigenfunction associated to the zero eigenvalue is the constant function on Γ.

The eigenfunctions are $\varphi_n(\theta) = e^{in\theta}$ for $n \in \mathbb{Z}$ and we have

$$\Lambda_{\mathcal{S}_0}\varphi_n = \frac{2}{\sqrt{\pi}}\frac{\partial}{\partial\theta_x}\int_\Gamma \sqrt{R}\left((\cos(\theta)-\cos(\theta_x))^2 + (\sin(\theta)-\sin(\theta_x))^2\right)^{1/4} \frac{\partial e^{in\theta}}{\partial\theta} R\, d\theta$$

$$\Lambda_{\mathcal{S}_0}\varphi_n = -\frac{2R^{3/2}n^2}{\sqrt{\pi}} e^{in\theta_x} I_n,$$

with $I_n = \int_0^{2\pi} \sqrt{2\left|\sin(\frac{\tilde\theta}{2})\right|}\, e^{in\tilde\theta}\, d\tilde\theta$ where we made the change of variable $\tilde\theta = \theta - \theta_x$. Therefore, we have obviously

$$\lambda_n = -\frac{2R^{3/2}n^2}{\sqrt{\pi}} I_n.$$

We want to prove that $I_{n\geq 1} < 0$. The parity of the integrand in I_n yields

$$I_n = 2\int_0^{\pi} \sqrt{2\left|\sin\left(\frac{\tilde\theta}{2}\right)\right|} \cos(n\tilde\theta)\, d\tilde\theta.$$

Let $f(t), t \in [0, \pi]$ be a positive concave increasing function, and we set $I_n(f) = \int_0^{\pi} f(t)\, \cos(nt)\, dt$. Integration by parts yields

$$\begin{aligned} I_n(f) &= -\frac{1}{n}\int_0^{\pi} f'(t)\sin(nt)\, dt \\ &= -\frac{1}{n^2}\int_0^{n\pi} f'\left(\frac{t}{n}\right)\sin(t)\, dt \\ &= -\frac{1}{n^2}\sum_{k=0}^{n-1}\int_{k\pi}^{(k+1)\pi} f'\left(\frac{t}{n}\right)\sin(t)\, dt \\ &= -\frac{1}{n^2}\sum_{k=0}^{n-1} J_k. \end{aligned}$$

If $n = 1$, obviously $I_n(f) \leq 0$. In fact, we only need to prove that for all even numbers k in $[0, n-2]$, the quantity $J_k + J_{k+1}$ is a positive real number. Let $f'_{k+j} = f'(\frac{k+j}{n})$ and set k even, then $\sin(t) \geq 0$ and

$$\begin{cases} J_k \geq \displaystyle\int_{k\pi}^{(k+\frac{1}{2})\pi} f'_{k+\frac{1}{2}}\sin(t)\, dt + \int_{(k+\frac{1}{2})\pi}^{(k+1)\pi} f'_{k+1}\sin(t)\, dt \\ J_{k+1} \geq \displaystyle\int_{(k+1)\pi}^{(k+\frac{3}{2})\pi} f'_{k+1}\sin(t)\, dt + \int_{(k+\frac{3}{2})\pi}^{(k+2)\pi} f'_{k+\frac{3}{2}}\sin(t)\, dt. \end{cases}$$

Finally,

$$J_k + J_{k+1} \geq f'_{\frac{1}{2}} - f'_{\frac{3}{2}} \geq 0$$

with strict inequality if f' is decreasing. We can easily check that $f(t) = 2\sqrt{2\sin(\frac{t}{2})}$ complies with all the hypotheses and for all $n \geq 1$, $I_n < 0$. The eigenspace associated to $\lambda_0 = 0$ is spanned by $\varphi_0(\theta) = 1$ and $\lambda_{n\geq 1} > 0$ which concludes the proof. □

It is not yet sufficient to prove that it is an isomorphism on any contour. In fact, we will use a weakened hypothesis on $\Lambda_{\mathcal{S}_0}$ but we still suppose that Γ is a $\mathcal{C}^\infty$ curve.

Theorem 4.1. *Let Γ be a $\mathcal{C}^\infty$ curve, the functional space V and $\Lambda_{\mathcal{S}_0}$ being defined as in Proposition 4.1. Let also $(\mathcal{T}_l)_{l\in\mathbb{N}}$ and $(V_l)_{l\in\mathbb{N}}$ be the sequences of meshes and nested approximation spaces introduced in Section 2 such that the function $v = 1$ belongs to V_l, then there exists a rank l_0 such that for all $l \geq l_0$, the a posteriori error estimate for $|||u - u_l|||$ defined by*

$$\eta_{\Lambda_{\mathcal{S}_0}} = \|\Lambda_{\mathcal{S}_0} r_l\|_0, \tag{18}$$

is reliable, efficient, local and asymptotically exact.

Proof. We can decompose $\Lambda_{\mathcal{S}_0}$ as the sum of an isomorphism $\Lambda_0 : V \to L^2(\Gamma)$ and a compact perturbation $K : V \to L^2(\Gamma)$. For example, by construction, $\Lambda_{\mathcal{S}_0}$ has the same principal symbol as $\mathcal{S}_0^{-1/2}$ which is an isomorphism on V and consequently, we can take $\Lambda_0 = \mathcal{S}_0^{-1/2}$ and $K = \Lambda_{\mathcal{S}_0} - \mathcal{S}_0^{-1/2}$. More generally, the structure of the principal symbol of $\Lambda_{\mathcal{S}_0}$ implies that the latter is a strongly elliptic operator and consequently, it verifies a Garding inequality (see [22]).

The hypothesis $v = 1 \in V_l$ implies that $r_l \in V$ and we have

$$\begin{aligned} \|\Lambda_{\mathcal{S}_0} r_l\|_0^2 &= ((\Lambda_0 + K)r_l, (\Lambda_0 + K)r_l) \\ &= \langle \Lambda_0^\star \Lambda_0 r_l, r_l\rangle_{-1/2,1/2} + \langle \tilde K r_l, r_l\rangle_{-1/2,1/2}, \end{aligned}$$

where $\tilde K = \Lambda_0^\star K + K^\star \Lambda_0 + K^\star K$ is compact.

Since Λ_0 is an isomorphism, there exist two constants $C_1,\ C_2 > 0$ such that

$$\left|C_1 \|r_l\|_{1/2}^2 - \|\tilde{K} r_l\|_{-1/2}\|r_l\|_{1/2}\right| \leq \|\Lambda_{s_0} r_l\|_0^2 \leq C_2 \|r_l\|_{1/2}^2 + \|\tilde{K} r_l\|_{-1/2}\|r_l\|_{1/2},$$

and we would like $\|\tilde{K} r_l\|$ to converge faster than $\|r_l\|_{1/2}$ as $l \to \infty$. Using Lemma 2.2 and the fact that $\|r_l\|_{1/2}$ is a reliable and efficient *a posteriori* error estimate of the norm of the error $|||e_l|||$, *i.e.*, there exist $\beta_1,\ \beta_2 > 0$ such that $\beta_1|||e_l||| \leq \|r_l\|_{1/2} \leq \beta_2|||e_l|||$, we have

$$\delta_l := \frac{\|\tilde{K} r_l\|_{-1/2}}{\|r_l\|_{1/2}} = \frac{\|\tilde{K}\mathcal{A} e_l\|_{-1/2}}{\|r_l\|_{1/2}} \leq \frac{\|\tilde{K}\mathcal{A} w_l\|_{-1/2}}{\beta_1} \xrightarrow{l\to\infty} 0.$$

Finally, there exist two constants $C_3 > 0$ and $C_4 > 0$ and a rank $l_0 \in \mathbb{N}$ such that for all $l \geq l_0$,

$$C_3|||e_l||| \leq \|\Lambda_{s_0} r_l\|_0 \leq C_4|||e_l|||,$$

i.e., the reliability and the efficiency where $C_3 = \beta_1 C_1 - \delta_l$ and $C_4 = \beta_2 C_2 + \delta_l$. The asymptotic exactness is a result from Proposition 3.1. □

Remark 4.1. The rank l_0 introduced in Theorem 4.1 corresponds to the moment when the compact parts resulting from the decomposition $\Lambda_{s_0} = \Lambda_0 + K$ are under control.

4.2. Construction of $\Lambda_{\mathcal{N}_0}$

We construct the operator Λ associated to $\mathcal{N}_0$. We will follow the same approach as for Λ_{s_0}. We already know from (15) the principal symbol of $\Lambda_{\mathcal{N}_0}$. We seek the associated Schwartz-kernel. From formula (7.1.39) in [22],

$$\begin{aligned} k(x,z) &= \frac{\sqrt{2}}{2\pi}\int_{\mathbb{R}} \frac{e^{i\xi z}}{\sqrt{|\xi|}}\, d\xi \\ &= \frac{1}{\sqrt{2}\pi}\left(\lim_{\xi\to\infty} \frac{\sqrt{\pi}\,\mathrm{erf}(\sqrt{-iz}\sqrt{\xi})}{\sqrt{-iz}} + \lim_{\xi\to-\infty} \frac{\sqrt{\pi}\,\mathrm{erf}(\sqrt{iz}\sqrt{-\xi})}{\sqrt{iz}}\right) \\ &= \sqrt{\frac{2}{\pi}}\Re\left(\frac{1}{\sqrt{iz}}\right) \\ &= \sqrt{\frac{2}{\pi}}\sqrt{\frac{|z|}{2}}\frac{1}{|z|} \\ &= \frac{1}{\sqrt{\pi}}\frac{1}{\sqrt{|z|}}. \end{aligned}$$

We define

$$\boxed{\Lambda_{\mathcal{N}_0} u(x) = \frac{1}{\sqrt{\pi}}\int_\Gamma \frac{u(y)}{\sqrt{|x-y|}}\, d\gamma_y}. \tag{19}$$

We have a theorem similar to Theorem 4.1.

Theorem 4.2. *Let Γ be a $\mathcal{C}^\infty$ curve, and $\Lambda_{\mathcal{N}_0}$ as defined in (19). Let also $(\mathcal{T}_l)_{l\in\mathbb{N}}$ and $(V_l)_{l\in\mathbb{N}}$ be the sequences of meshes and nested approximation spaces introduced in Section 2, then there exists a rank l_0 such that for all $l \geq l_0$, the a posteriori error estimate for $|||u - u_l|||$ defined by*

$$\eta_{\Lambda_{\mathcal{N}_0}} = \|\Lambda_{\mathcal{N}_0} r_l\|_0,$$

is reliable, efficient, local and asymptotically exact.

Proof. The proof is carried in the same fashion as for Theorem 4.1. □

5. Numerical examples

In this section we aim at validating the properties of Λ_{s_0} and $\Lambda_{\mathcal{N}_0}$. We only consider the exterior Dirichlet and Neumann problems. The curve Γ is closed. In this paper we suppose that the incident wave u_i is a plane wave propagating along the $-\mathbf{e}_x$ axis. For all the simulations, the wave number is set to

$$k = 15.$$

We focus on two geometries: a circle with radius $R = 0.9$ and a square with side length $a = 1$. The justifications for the choice of these geometries are given in the corresponding subsections.

The initial meshes contain 20 elements which correspond to approximately 2 elements per wavelength. This is really low as the rule of thumb recommends both at least 6 elements per wavelength and additional refinement at the edges/corners [25]. We choose such a low initial discretization in order to "get the estimate's back against the wall".[1]

For each case, the autoadaptive refinement algorithm is guided using η_Λ. The value of η_Λ is compared to the value of some estimates of the literature:

- The residual-based estimate by C. Carstensen et al. [10,11], written η_{r_h}.
- An averaging-based estimate by D. Praetorius et al. [12,13]. When the projector is the classical L^2 projector, we write the corresponding estimate $\eta_{\Pi_{L^2}}$. In the case of Eq. (1), we also tried the Galerkin projection and the corresponding estimate is written η_{Π_G}.
- The reference solution which can either be the exact solution when available (on the circle), or an "exact estimate". The latter consists in comparing the solution u_l with the solution $\widehat{u}_l$ for some refinement $\widehat{\mathcal{T}}_l$ of $\mathcal{T}_l$.

The rest of this section is organized as follows: we first give informations on the implementation of the BEM and the different estimates. We then explain the refinement algorithm which is used. Finally, we introduce the test cases and produce the result for the estimate $\eta_{\Lambda_{\mathcal{S}_0}}$ and for $\eta_{\Lambda_{\mathcal{N}_0}}$.

5.1. Implementation of the BEM and the estimates

The approximation/test space for Eq. (3) is chosen to be $V_l = \mathcal{P}^0(\mathcal{T}_l)$, the space of constant functions on $\mathcal{T}_l$. Assuming that the mesh is quasi-uniform and that the exact solution is smooth enough, then the best possible convergence rate with respect to the size of the elements can be estimated using the Bramble–Hilbert lemma (see [26, Theorem 4.1.3]) from the polynomial degree of the approximation spaces. We expect the *best possible* convergence rate

$$\|e_l\|_{-1/2} = \mathcal{O}(h_l^{3/2}) = \mathcal{O}(N_{\text{elem}}^{-3/2})$$

where N_{elem} is the number of elements in $\mathcal{T}_l$. The reason why the convergence rate is expressed with respect to N_{elem} is that the mesh size is not relevant anymore. On the contrary, the computation cost is directly linked to N_{elem}. We only *hope* that by using autoadaptive refinement we are able to obtain the convergence rate for a smooth solution, even if it is not.

For Eq. (4), the approximation/test space is $V_l = \mathcal{P}^1(\mathcal{T}_l)$ the continuous space of linear functions on $\mathcal{T}_l$. As for Eq. (3), we expect $\|e_l\|_{1/2} = \mathcal{O}(h_l^{3/2}) = \mathcal{O}(N_{\text{elem}}^{-3/2})$.

The BEM matrix elements are integrated using semi-analytical integration. For couples of elements for which the integral is singular, the kernel is decomposed in a singular part and a regular part. The regular part is integrated using classical Gauss–Legendre quadrature rules.

The singular part consists in integrating two times a logarithmic function times some polynomial. The inner integral is computed analytically while the outer integral is computed using once again a Gauss–Legendre quadrature rule.

However, it has been noticed that when the degree of refinement is high, the numerical solution has instabilities. In that case, one must increase the number of quadrature points.

The implementation of the estimates depends on the ability to compute the residual. The basis remains the same: we compute a polynomial approximation $\mathbf{R}_l$ of the residual, we assemble the matrix $\mathbf{L}$ corresponding to the variational formulation associated to the operator Λ, we assemble the classical L^2-mass matrix, and we compute a polynomial approximation of Λr_l under the form

$$\mathbf{E} = \mathbf{M}^{-1}\mathbf{L}\mathbf{R}_l.$$

The estimate is then computed as $\eta_\Lambda^2 = \mathbf{E}^{\mathrm{T}}\mathbf{M}\mathbf{E}$.

For both Eqs. (1) and (2), the residual is projected using a classical L^2 projection on a polynomial space of higher order. The main difference lies in the mesh on which the residual is projected.

In the case of Eq. (1), the projection on the same mesh $\mathcal{T}_l$ fails to be accurate and leads to a poor behavior for the convergence with a lot of oscillations. To remedy this problem, we must project the residual on a uniform refinement $\widehat{\mathcal{T}}_l$ of $\mathcal{T}_l$. To achieve good accuracy, we had to refine $\mathcal{T}_l$ at least three times (each "old" segment contains 2^3 new segments)! The projection space is then $\mathcal{P}^1(\widehat{\mathcal{T}}_l)$.

In the case of Eq. (2), the projection on the mesh $\mathcal{T}_l$ proves sufficient to achieve a good accuracy. The projection space is $\mathcal{P}^2(\mathcal{T}_l)$ which is the space of piecewise quadratic, globally continuous, functions.

The entries of the matrix $\mathbf{L}$ are computed analytically when we consider the integration of an element over itself. In the other cases, classical Gauss–Legendre quadrature are sufficient.

[1] If the initial number of elements is too low, the estimate "may not detect" the oscillations and yields a very low error.

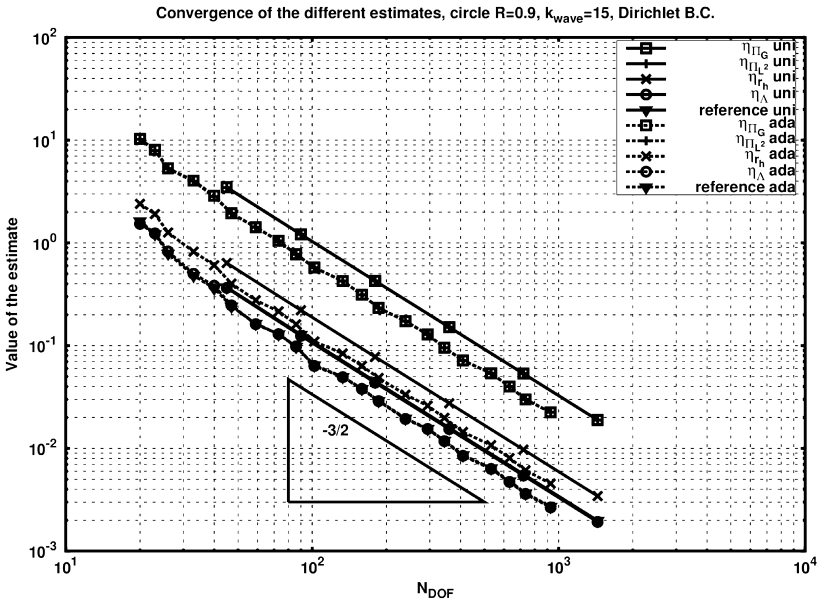

Fig. 2. Convergence of different estimates, circle $R = 0.9$, $k = 15$, Dirichlet b.c.

5.2. The autoadaptive refinement algorithm

The sequence of meshes $(\mathcal{T}_l)_{l\in\mathbb{N}}$ is generated using the autoadaptive loop described in Fig. 1. The criterion used for the marking is the Dörfler marking (see e.g. [16]) with parameter θ_{d}. We mark the elements using the squared indicator, *i.e.*, we refine the minimum set $\mathcal{M}(\mathcal{T}_l)$ of elements $\tau \in \mathcal{T}_l$ such that

$$\theta_{\mathrm{d}} \sum_{\tau\in\mathcal{T}_l} \eta^2_{\Lambda,\tau} \leq \sum_{\tau\in\mathcal{M}(\mathcal{T}_l)} \eta^2_{\Lambda,\tau}. \tag{20}$$

In other words, we mark the elements of $\mathcal{T}_l$ contributing the most to $100 \cdot \theta_{\mathrm{d}}\%$ of the total squared error. If θ_{d} is close to 0, only a few elements are refined. On the contrary, θ_{d} close to 1 induces "nearly uniform" refinement. In the following we choose $\boxed{\theta_{\mathrm{d}} = 0.5}$ as it seems to be a good compromise.

The elements being linear, the refinement is carried out by bisecting each element.

The algorithm stops when a prescribed number of elements in the mesh is reached.

5.3. Numerical application — circle with radius $R = 0.9$

The circle is probably the most simple geometry. The exact solution for both Eqs. (1) and (2) is perfectly smooth and the convergence rate for uniform refinement is already the best possible convergence rate. This test case fulfills all the hypotheses of the development made in the Sections 2–4.

The convergence curves for Eq. (1) are presented in Fig. 2. The uniform convergence rate is already the best possible for uniform refinement and autoadaptive refinement only slightly improves the value of the error. We observe that the curves for $\eta_{\Lambda_{s_0}}$ and the reference overlap perfectly.

We observe the same behavior for Eq. (2) in Fig. 3. In that case, the improvement coming from autoadaptive refinement is negligible.

As expected, the estimate η_Λ behaves perfectly well on a smooth geometry. Unfortunately, smooth geometries are barely useful, nor met, in practical applications. We wish to know how the Λ-based estimate behaves when it is *pulled out of its theoretical environment*.

5.4. Numerical application — unit square

We choose now the geometry to be a square with side length $a = 1$. It is now a Lipschitz curve and we fail to meet the hypothesis for the development of Section 4. It is also known from the literature [27] that the solution in the case of the Dirichlet problem is singular at the corners while it is weakly continuous in the case of the Neumann problem. Consequently, the convergence rate is not the best possible when using uniform mesh refinement.

However, we expect that the estimates keep their properties in this more general case.

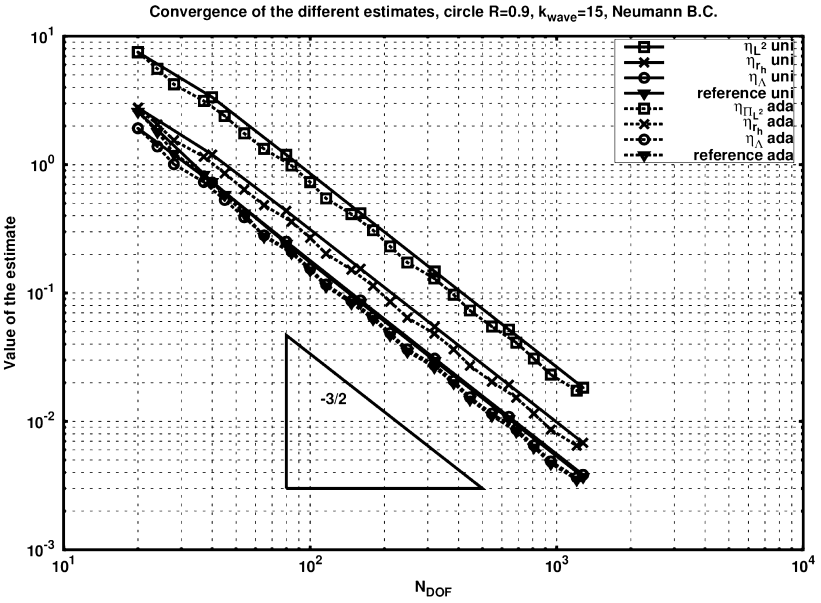

Fig. 3. Convergence of different estimates, circle $R = 0.9$, $k = 15$, Neumann b.c.

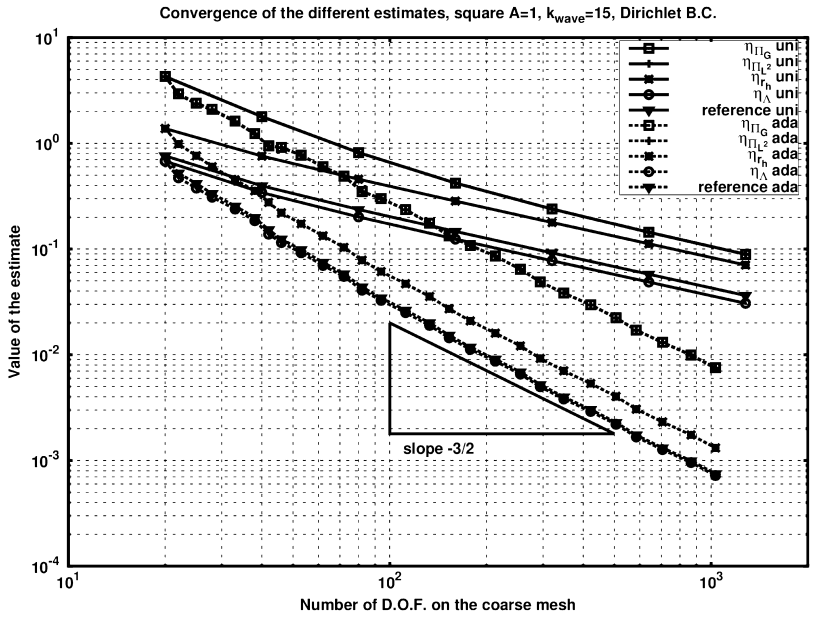

Fig. 4. Convergence of different estimates, square $a = 1$, $k = 15$, Dirichlet b.c.

The convergence curves for the Dirichlet problem are represented in Fig. 4. Uniform refinement is clearly suboptimal as the convergence rate is approximately[2] $\mathcal{O}(N_{\text{elem}}^{-0.66})$. The curves for $\eta_{\Lambda_{\delta_0}}$ and the reference overlap. It means that the "exact" error in the Galerkin norm is also accurately estimated by $\eta_{\Lambda_{\delta_0}}$. The autoadaptive algorithm is also efficiently guided by $\eta_{\Lambda_{\delta_0}}$ since the convergence rate for autoadaptive refinement is the best possible.

We make the same observation for the Neumann problem, in Fig. 5, for which the error is accurately estimated and the convergence rate is the best possible.

2 Using [27] and the Bramble–Hilbert lemma, we can prove this value.

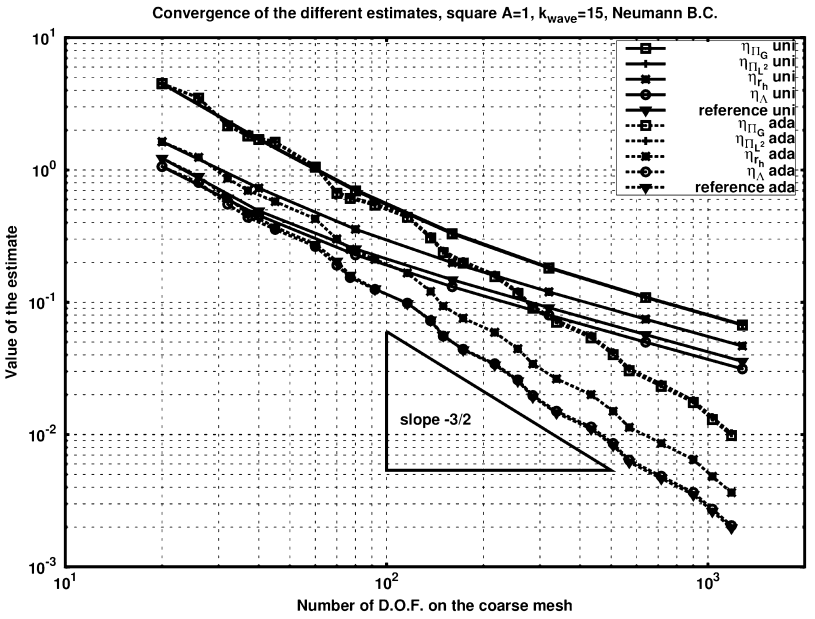

Fig. 5. Convergence of different estimates, square $a = 1$, $k = 15$, Neumann b.c.

6. Conclusion

We introduced a new *a posteriori* error estimate for which we were able to prove the reliability and efficiency when Γ is a $\mathcal{C}^\infty$ curve for both Eqs. (1) and (2). In this case, the Λ-estimate is asymptotically exact for any Γ with respect to the Galerkin norm of the error in the sense that it is exact up to higher order terms. This is confirmed by numerical simulations on the circle. We also verify numerically that it is reliable, efficient and asymptotically exact on Γ with corners, but we are not yet able to prove it.

Its main advantages are that it does not require the computation of the solution on a finer mesh (as required by the averaging techniques) or the use of complementary functional subspaces (see [28]). The first tricky point will be the accurate computation of the residual which can be costly. However this can be accelerated with a fast-multipole algorithm. The second difficulty will be the computation of the Λ-operator as it may require the computation of singular integrals.

In this paper, the Λ-estimate has been introduced for oscillatory problems but it remains of course valid for the classical problem of the Laplace equation. Much better, we provide a generic pattern for the construction of an *a posteriori* error estimate for the BEM in general. The "only" difficulty will be to find an appropriate Λ-operator.

We understand that the use of an integral operator for *a posteriori* estimation is costly. In fact, it is totally impractical as soon as we are dealing with 3D-acoustics since it requires specific integration technique on triangles for the singular kernels. Consequently, we are currently investigating the use of Λ under the form $\Lambda \equiv \sqrt{2}\,(\mathrm{Id} - \Delta)^{\pm 1/4}$ for which it has already been proven that it is an isomorphism on generic Lipschitz boundaries and for which it is easier to define a behavior in the case of screen problems.

Acknowledgments

This work is funded by the Ministère français de la Défense and the Agence Nationale de la Recherche (RAFFINE project, ANR-12-MONU-0021).

References

[1] J. Carrier, L. Greengard, V. Rokhlin, A fast adaptive multipole algorithm for particle simulations, SIAM J. Sci. Stat. Comput. 9 (4) (1988) 669–686.
[2] W. Hackbusch, Hierarchical Matrices: Algorithms and Analysis, Vol. 49, Springer, Berlin, Heidelberg, 2015.
[3] J.-C. Nédélec, Acoustic and Electromagnetic Equations: Integral Representations for Harmonic Problems, in: Applied Mathematical Sciences, Springer, New-York, 2001.
[4] B. Faermann, Local a posteriori error indicators for the Galerkin discretization of boundary integral equations, Numer. Math. 79 (1998) 43–76.
[5] B. Faermann, Localization of the Aronszajn–Slobodeckij norm and application to adaptive boundary element methods. Part I. The two-dimensional case, IMA J. Numer. Anal. 20 (2) (2000) 203–234.
[6] B. Faermann, Localization of the Aronszajn–Slobodeckij norm and application to adaptive boundary element methods. Part II. The three-dimensional case, Numer. Anal. 92 (2002) 467–499.
[7] M. Maischak, P. Mund, E.P. Stephan, Adaptive multilevel BEM for acoustic scattering, Comput. Methods. Appl. Mech. Engrg. 150 (1997) 351–367.
[8] J.T. Chen, K.H. Chen, C.T. Chen, Adaptive boundary element method for time-harmonic exterior acoustics in two dimensions, Comput. Methods Appl. Mech. Engrg. 191 (2002) 3331–3345.

[9] R.H. Nochetto, B. Stamm, A posteriori error estimates for the electric field integral equation on polyhedra, 2012. ArXiv e-prints arXiv:1204.3930.
[10] C. Carstensen, An a posteriori error estimate for a first-kind integral equation, Math. Comp. 66 (217) (1997) 139–155.
[11] C. Carstensen, M. Maischak, D. Praetorius, E.P. Stephan, Residual-based a posteriori error estimate for hypersingular equation on surfaces, Numer. Math. 97 (3) (2004) 397–425.
[12] C. Carstensen, D. Praetorius, Averaging techniques for the effective numerical solution of symm's integral equation of the first kind, SIAM J. Sci. Comput. 27 (4) (2006) 1226–1260.
[13] C. Carstensen, D. Praetorius, Averaging techniques for a posteriori error control in finite element and boundary element analysis, in: O. Steinbach, M. Schanz (Eds.), Boundary Element Analysis, Vol. 29, 2007, pp. 29–59.
[14] M. Feischl, T.F. Führer, N. Heuer, M. Karkulik, D. Praetorius, Adaptive boundary element methods: A posteriori error estimators, adaptivity, convergence, and implementation, Arch. Comput. Methods Eng. 22 (3) (2014) 309–389.
[15] M. Feischl, M. Karkulik, J.M. Melenk, D. Praetorius, Quasi-optimal convergence rate for an adaptive boundary element method, SIAM J. Numer. Anal. 51 (2) (2013) 1327–1348.
[16] C. Carstensen, M. Feischl, M. Page, D. Praetorius, Axioms of adaptivity, Comput. Methods Appl. Math. 67 (6) (2014) 1195–1253.
[17] W. McLean, Strongly Elliptic Systems and Boundary Integral Equations, Cambridge University Press, 2000.
[18] A. Bespalov, A. Haberl, D. Praetorius, Adaptive FEM with coarse initial mesh guarantees optimal convergence rates for compactly perturbed elliptic problems, Comput. Methods Appl. Mech. Engrg. 317 (2017) 318–340.
[19] M. Feischl, T. Führer, D. Praetorius, Adaptive FEM with optimal convergence rates for a certain class of nonsymmetric and possibly nonlinear problems, SIAM J. Numer. Anal. 52 (2) (2014) 601–625.
[20] X. Antoine, M. Darbas, Generalized combined field integral equations for the iterative solution of the three-dimensional Helmholtz equation, ESAIM Math. Model. Numer. Anal. 41 (1) (2007) 147–167.
[21] D. Levadoux, F. Millot, S. Pernet, A well-conditioned boundary integral equation for transmission problems of electromagnetism, J. Integral Equations Appl. 27 (3) (2015) 431–454.
[22] G.C. Hsiao, W.L. Wendland, Boundary Integral Equations, in: Applied Mathematical Sciences, Springer, Berlin, Heidelberg, 2008.
[23] I.H. Sloan, A. Spence, The Galerkin method for integral equations of the first kind with logarithmic kernel: theory, IMA J. Numer. Anal. 8 (1) (1988) 105–122.
[24] M. Lecouvez, F. Collino, P. Joly, B. Stupfel, Quasi-local transmission conditions for non-overlapping domain decomposition methods for the Helmholtz equation, C. R. Phys. 15 (5) (2014) 403–414.
[25] S. Marburg, B. Nolte, Computational Acoustics of Noise Propagation in Fluids — Finite and Boundary Element Method, Springer, Berlin, Heidelberg, 2008 (Chapter 12).
[26] P.G. Ciarlet, Finite Element Method for Elliptic Problems, Society for Industrial and Applied Mathematics, Philadelphia, PA, USA, 2002.
[27] P. Grisvard, Singularities in Boundary Value Problems, in: Recherches en Mathématiques Appliquées, Masson, 1992.
[28] J. Jou, J.-L. Liu, A posteriori boundary element error estimation, J. Comput. Appl. Math. 106 (1) (1999) 1–19.